UC Irvine
UC Irvine Previously Published Works

Title

Acceleration and spatial rheology of Larsen C Ice Shelf, Antarctic Peninsula

Permalink

https://escholarship.org/uc/item/7qr5m554

Journal

Geophysical Research Letters, 38(9)

ISSN

0094-8276

Authors

Khazendar, A
Rignot, E
Larour, E

Publication Date

2011-05-16

DOI

10.1029/2011gl046775

Copyright Information

Peer reviewed

Acceleration and spatial rheology of Larsen C Ice Shelf, Antarctic Peninsula

A. Khazendar,[1] E. Rignot,[1,2] and E. Larour[1]

[1]   The disintegration of several Antarctic Peninsula ice shelves has focused attention on the state of the Larsen C Ice Shelf. Here, we use satellite observations to map ice shelf speed from the years 2000, 2006 and 2008 and apply inverse modeling to examine the spatial pattern of ice-shelf stiffness. Results show that the northern half of the ice shelf has been accelerating since 2000, speeding up by 15% between 2000 and 2006 alone. The distribution of ice stiffness exhibits large spatial variations that we link to tributary glacier flow and fractures. Our results reveal that ice down-flow from promontories is consistently softer, with the exception of Churchill Peninsula where we infer a stabilizing role for marine ice. We conclude that although Larsen C is not facing imminent collapse, it is undergoing significant change in the form of flow acceleration that is spatially related to thinning and fracture. **Citation:** Khazendar, A., E. Rignot, and E. Larour (2011), Acceleration and spatial rheology of Larsen C Ice Shelf, Antarctic Peninsula, *Geophys. Res. Lett.*, *38*, L09502, doi:10.1029/2011GL046775.

1.   Background

[2]   The Larsen C Ice Shelf covers an area of 55,000 km^2 [*Riedl et al.*, 2004] between Jason Peninsula in the north and Hearst Island in the south (Figure 1a), which makes it 5 times larger than the 1995 extent of Larsen B Ice Shelf. That was the year when Larsen B started an irreversible front retreat that culminated in its abrupt disintegration in March 2002. Such rapid demise of an ice shelf that had existed throughout the Holocene and earlier disintegrations of other shelves on the Antarctic Peninsula raised the question of whether Larsen C could meet a similar fate. These events demonstrated the link between the removal of ice shelves and acceleration of their tributary glaciers [e.g., *Rignot et al.*, 2004]. Hence, with a catchment area of 27,000 km^2 [*Riedl et al.*, 2004] drained by steep and narrow glaciers that descend from the high plateau and flow into the shelf through approximately 10 inlets at which the ice shelf is thickest (Figure 1b), the removal of Larsen C will likely result in the acceleration of these glaciers and a significant increase in continental ice volume discharge into the ocean.

[3]   At present, the areal extent and surface morphology of Larsen C do not suggest major change, but other aspects presage possible destabilization. Thus, since 1986–1989 the ice shelf had no major calving events [*Riedl et al.*, 2004; *Cook*

and Vaughan, 2010], overall surface features over a period of 40 years show few changes [*Glasser et al.*, 2009], and modeled flow velocities and the corresponding stress distribution indicate that it is stable at the moment [*Jansen et al.*, 2010]. On the other hand, satellite radar altimetry for the period 1992–2001 indicates that Larsen C lowered by up to 0.27 m a^{-1}, especially in the north [*Shepherd et al.*, 2003]. Laser altimetry and ice thickness data obtained in November 2002 and November 2004 during the CECS/NASA airborne campaigns show a higher surface elevation drop rate of 0.37 m a^{-1} during the 2-year period. R. Thomas (personal communication, 2009) used these data to calculate the air content of firn after correcting surface elevations for the local geoid (EGM96) and tides, finding a northward decrease in air content. This is consistent with warmer conditions there and more melting, indicating that the ice shelf is becoming less permeable to meltwater, an occurrence that has been proposed as a precursor to ice shelf-breakup [*Rott et al.*, 1996; *Scambos et al.*, 2000]. Putting the thinning and increased surface melting in the context of atmospheric warming in the Antarctic Peninsula over the past century, which was 5–6 times larger than the global average, emphasizes the uncertain future of the ice shelf. Indeed, the −9°C average surface temperature isotherm, suspected of being the northern limit of ice-shelf viability [*Morris and Vaughan*, 2003], already crosses the northern edge of Larsen C.

[4]   In this study we investigate two essential elements to elucidating the current state of Larsen C: its flow regime and its spatial distribution of rheology.

2.   Speed Fields and Flow Acceleration

[5]   We obtain the velocity field of Larsen C by applying a speckle tracking technique on 3 synthetic-aperture radar interferometry (InSAR) data sets. The speeds for Oct.-Dec. 2008 (Figure 2) and Oct.-Dec. 2006 are from ALOS PALSAR InSAR data with uncertainties of ±5 and ±10 m a^{-1}, respectively (uncertainty estimates were based on the measured standard deviation in ice speed over stagnant, yet ice covered, areas). The speeds for Sept.-Oct. 2000 are from Radarsat-1 InSAR data with uncertainty of ±10 m a^{-1}. This motion field has several gaps in the southern part surrounded by areas with high noise, hence we cannot draw conclusions on speed changes there. The speeds are averaged over the 44-day (ALOS) and 24-day (Radarsat-1) repeat cycles hence making errors due to vertical tidal movements insignificant. Any seasonal effects are minimized by all data sets being from the Austral spring, and by the long periods over which displacement is calculated.

[6]   The motion fields exhibit the characteristic spatial pattern of embayed ice shelves [e.g., *Larour et al.*, 2005]. Speed increases from the grounding line to a maximum at the middle section of the ice front. A few lines of higher

[1]Jet Propulsion Laboratory, California Institute of Technology, Pasadena, California, USA.
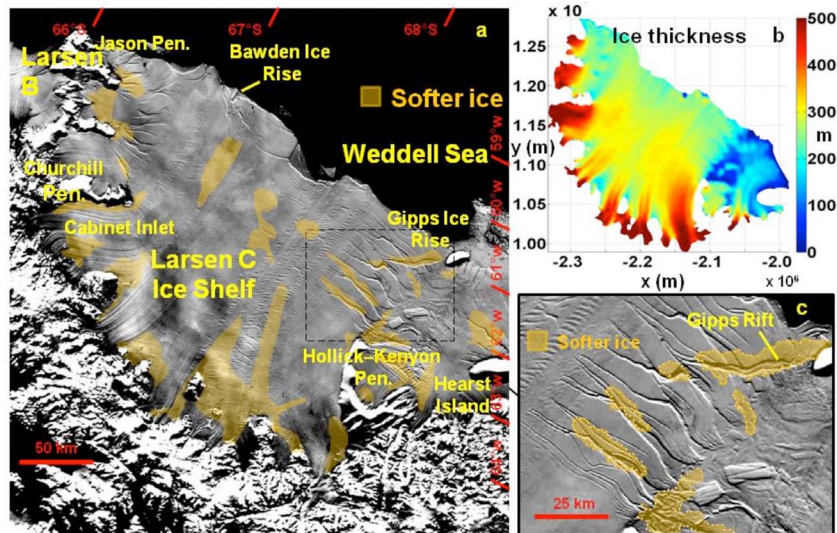[2]Earth System Science, University of California, Irvine, California, USA.

Figure 1. (a) MODIS mosaic of Antarctica image of Larsen C [*Haran et al.*, 2005], with approximate areas of the lowest flow parameter values from Figure 4 overlain to show their spatial correspondence to surface features. The dashed rectangle marks the location of Figure 1c. (b) The thickness distribution of Larsen C from *Griggs and Bamber* [2009], showing the thick tributary glaciers entering the ice shelf at the grounding line, and the much thinner zones between them located down-flow from promontories and peninsulas. Coordinates are polar stereographic (at 71°S secant plane, 0° meridian, WGS 84 ellipsoid), where x is easting and y is northing. (c) The outlines of rheology field areas having $B \leq 1.0 \times 10^8$ Pa s$^{1/3}$ (Figure 4) overlain on the backscatter image to show spatial relationship to fracture. With a maximum of 5 years between the acquisition dates of the backscatter mosaic [*Haran et al.*, 2005] and the speed field (Figure 2) used to infer rheology, and an ice flow speed in the area of about 500 m a^{-1}, the discrepancy between the locations of rifts and corresponding weakness zones is about 2.5 km.

speed gradients are also present, noticeably a 150–170 m a^{-1} speed difference over less than 5 km across sections of the Gipps rift. The rifts down-flow from the Hollick-Kenyon Peninsula and the Hearst Island rift also leave a discernible imprint on the motion field. Hence, the rather homogeneous speed flow pattern exhibits some irregularities that spatially correspond to the presence of fracture.

[7] Subtracting the year 2000 speed field from that of year 2006 reveals that over the 6-year interval the northern half of the ice shelf accelerated in places by 80 m a^{-1}, or 15%, near the ice front (Figure 3a), with similar rates of acceleration occurring upstream including the tributary glaciers. Speed change over the 2-year interval 2006–2008 shows acceleration continuing at around 2–4% near the front and in the central part, with higher rates of 6–8% in the Inlet Cabinet (Figure 3b). The southern edge of the acceleration area is bounded by the line of high speed gradient of the Gipps rift (Figure 3b). These speed-ups are compatible with the observed recent advance of the ice-shelf front [*Cook and Vaughan*, 2010], except for a calving event in January 2005 south of Bawden Ice Rise (Figure 1a), captured by MODIS imagery (http://nsidc.org/cgi-bin/new/iceshelves_images.pl), that could have weakened contact with the ice rise hence contributing partially to the observed acceleration.

[8] The change we detect in tributary glacier speeds is unlike the evolution of pre-disintegration Larsen B, where tributary glaciers did not appear to respond to the acceleration of the ice shelf [*Rignot et al.*, 2004].

3. Rheology and Fracture

[9] The flow parameter, B, is the proportionality coefficient between deviatoric stress and strain rate in Glen's flow law and therefore a measure of ice stiffness. The value of B depends on ice temperature, fabric and impurity and water content. Higher B values indicate stiffer ice. Here, we infer the rheology field by applying an inverse method that seeks
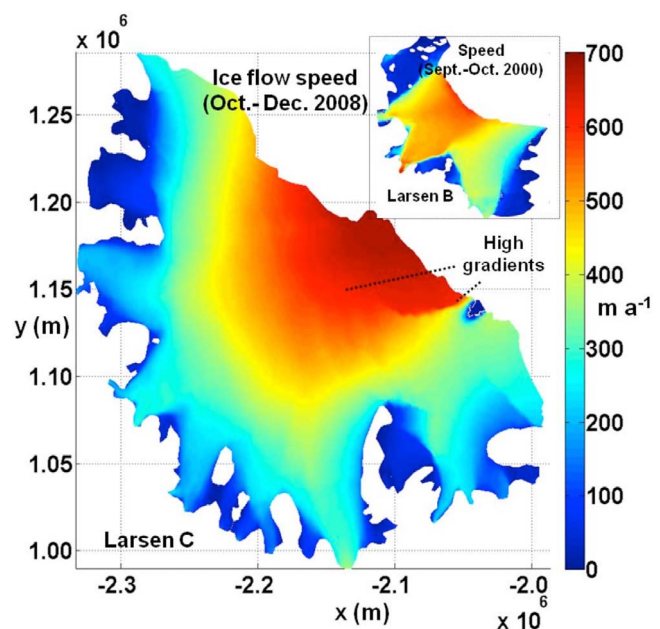

Figure 2. Ice flow speeds of Larsen C obtained for Oct.–Dec. 2008, completed with tracks from Oct.-Nov. 2007, from ALOS PALSAR data. The inset shows to the same scale the speed of Larsen B Ice Shelf for Sept.-Oct. 2000 measured by InSAR from Radarsat-1 data [*Khazendar et al.*, 2007].
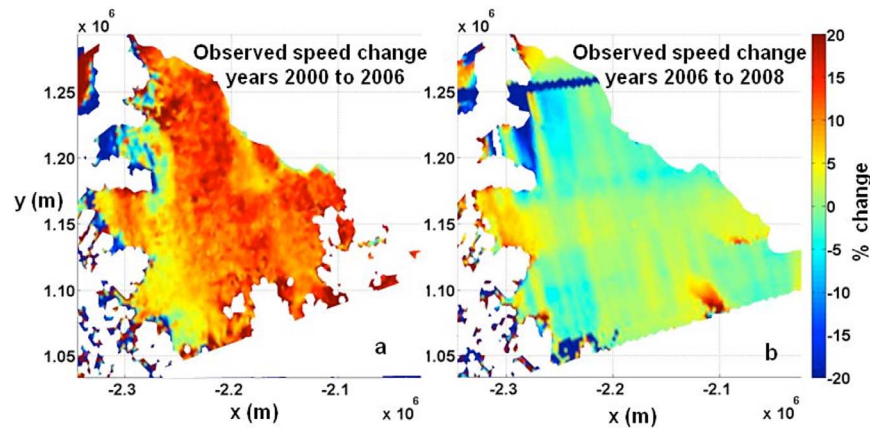
Figure 3. The percentage of speed change from (a) year 2000 to year 2006 relative to year 2000, and (b) from year 2006 to year 2008 relative to year 2006, in areas where speeds exceed 25 m/yr.

a depth-averaged spatial distribution of the flow parameter. The process is constrained by observations of ice thickness, grounding line and ice-front positions and ice-shelf surface velocity. Observed velocities are imposed at the grounding line and along Gipps Ice Rise. The model is initiated with a uniform B value producing a first estimate of the misfit between modeled and observed velocities. Iterations follow with modified spatial distributions of B until misfit variation stabilizes. The forward and inverse models are based on those by *Rommelaere and MacAyeal* [1997] with modifications by *Larour et al.* [2005]. This is the same methodology we applied in our analyses of Larsen B and Brunt/Stancomb-Wills ice shelves [*Khazendar et al.*, 2007, 2009]. Ice-shelf thickness (Figure 1b) is provided by a 1-km grid, based on 1994–1995 ERS-1 radar altimetry data, from *Griggs and Bamber* [2009].

The authors corrected for firn density and tidal movement, and validated surface elevations with independent airborne RES data obtaining a random error of 36.1 m. These thickness data significantly improved our modeling results compared with earlier digital topography especially near the ice-shelf grounding zone. We determined the grounding line position from double differential radar interferometry (the difference of two interferograms spanning the same time interval but acquired at different epochs) using ERS-1/2 measurements from March 1996, with horizontal error of less than ±100 m.

[10] The rheology distribution obtained from the 2008 motion field (Figure 2) shows pronounced spatial variability (Figure 4). This result confirms the spatial complexity of ice-shelf stiffness. Furthermore, the spatial pattern of stiffness is not random. Thus, the advection of colder tributary
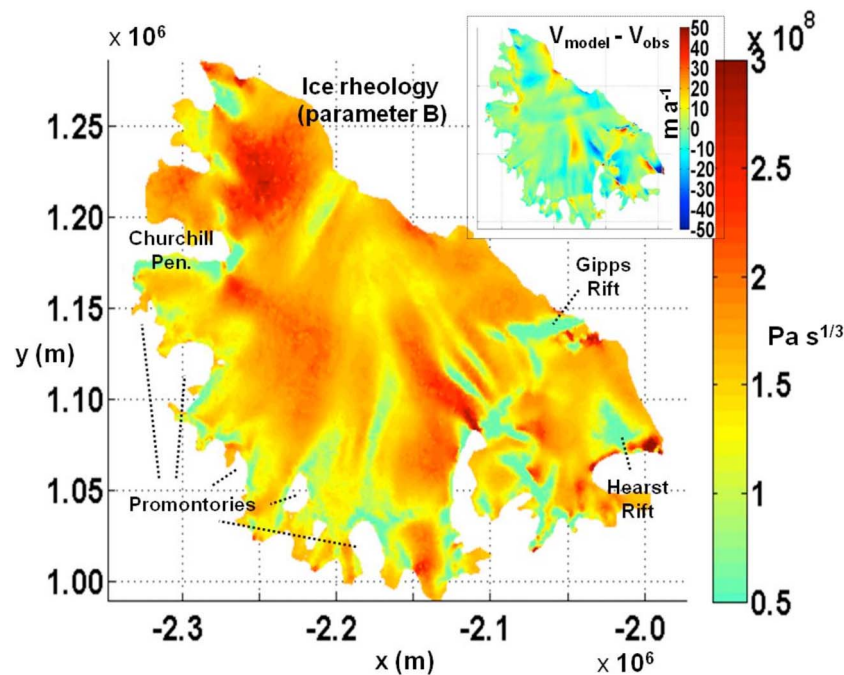

Figure 4. The rheology spatial distribution of Larsen C as obtained using the 2008 velocity field, naming some of the features mentioned in the text. The inset shows speed modeled using the rheology field minus the observed speed. Most of the ice shelf area has a discrepancy within ±15 m a^{-1}.

glacier ice onto the ice shelf is well represented by the vast expanses of stiffer ice originating at the grounding line and extending downstream for tens of kilometers. The areas of stiffer flow units are separated by prominent zones of weakness (Figure 4). Overlaying the outlines of the main zones of less stiff ice on the backscatter image in Figure 1a illustrates that these zones are consistently down-flow from the peninsulas and promontories located between the entry points of the tributary glaciers. The higher speed gradients that we observe there between fast-flowing and relatively stagnant ice (Figure 2) create strong lateral shearing typically associated with highly rifted and crevassed ice. A notable exception is the area down-flow from the Churchill Peninsula, which appears as one of the stiffer areas in the rheology field (Figure 4). There is also good spatial correspondence between certain prominent rifts, where there are strong gradients in speed as noted in the previous section, and areas of lower values in the inferred rheology. Specifically, the Gipps rift and other rifts in the wake of Hollick-Kenyon Peninsula clearly imprint the rheology field (Figure 4). Overlaying the outlines of these imprints on the backscatter image of that area (Figure 1c) illustrates their close spatial correspondence to the rifts. The concurrence of observed rifts, higher speed gradients and lower inferred ice stiffness is noteworthy. The continuum mechanics model we employ interprets the higher speed gradients associated with fracture as higher strain rates and hence lower inferred ice stiffness. We emphasize that this relates to already existing fractures, including rifts and bottom and surface crevasses, and that our model does not simulate the process of fracture opening. Field measurements and remote sensing have already linked the presence of ice-shelf fracture to higher strain rates and faster ice flow [*Rack et al.*, 2000; *Skvarca et al.*, 2004], as did numerical modeling in the specific case of Larsen C [*Jansen et al.*, 2010].

4. Discussion

[11] The results presented above offer several key insights into the state of Larsen C Ice Shelf. Our rheology field (Figure 4) provides evidence to support the presence of softer ice down-flow from promontories and peninsulas. The reduced stiffness of these suture zones of Larsen C, which separate flow units, was hypothesized by *Glasser et al.* [2009] to explain the remarkable rift-tip alignment such as that observed down-flow of the Hollick-Kenyon Peninsula (Figures 1a and 1c). On the other hand, *Holland et al.* [2009] explained it by the accumulation and subsequent advection of warmer, and hence less viscous, marine ice in the hollows located down-flow from the promontories. Yet, our work on Brunt/Stancomb-Wills Ice Shelf [*Khazendar et al.*, 2009] shows that the stiffness of ice mélange comprising marine ice was not as distinctly low in comparison with meteoric ice as it is of promontory ice here. Pertinently, we find that the ice down-flow from Churchill Peninsula is, exceptionally, among the stiffest in the ice shelf (Figure 4). This is precisely the area where *Holland et al.* [2009] simulated the most vigorous marine ice accumulation resulting from the confluence there of meltwater plumes, and where the backscatter image shows extensive ice mélange (Figure 1a). Hence, we propose that the lower stiffness of promontory ice is due in large part to the pres-

ence of fractures, only partially filled with marine ice, whereas the high stiffness of the Churchill Peninsula ice results from fracture being filled and healed [*Khazendar and Jenkins*, 2003] by abundant accretion of marine ice. This hypothesis is further supported by the relatively high speed gradients and lateral shear we observe near the grounding line between tributary glacier inflows and the surrounding ice (Figure 2), which are conducive to fracture formation in these particularly thinner areas of the ice shelf (Figure 1b). Indeed, *Jansen et al.* [2010] found that modeled stress intensities exceed fracture toughness and thus support crevasse opening down-flow of the promontories of Larsen C. A corollary of ice-shelf strengthening from substantial marine ice accretion is that weakening of marine ice layers as a result of changes in oceanic conditions could become a destabilizing factor, a point also pertinent to the second main finding of this work below.

[12] We detect an acceleration of the northern half of the ice shelf that appears to have been sustained over the 2000–2008 period. This is a sign of instability, akin to the 20% increase in the flow speed of Larsen B between 1996 and 2000 prior to its collapse [*Rignot et al.*, 2004]. The rheology field (Figure 4) reveals that the area of acceleration near the front (Figure 3b) is bounded by a contour that includes the Gipps rift and the band of soft ice that extends from one of the Hollick-Kenyon rifts northwards reaching into the central part of the ice shelf. This transverse line of weakness could be reflecting the presence of fractures–more likely bottom crevasses since surface fracturing is not apparent in the imagery–as ice-shelf temperature, fabric or water content are not expected to exhibit such spatial variation. Furthermore, this contour spatially corresponds closely to the outline of the area of higher speed gradients near the front indicated in Figure 2, making it unlikely to be a model artifact. It is also reminiscent in shape of the concave front Larsen B retreated to by the year 2000 [*Skvarca et al.*, 2004]. Our results reveal that the flow is accelerating in areas that overlap with those calculated by *Shepherd et al.* [2003] from satellite radar altimetry to exhibit the highest thinning rates between 1992 and 2001, presumably mainly from enhanced submarine melting. This hints at the possibility of marine ice in the suture zones being eroded as part of the general thinning hence weakening them and allowing faster ice flow. Replacement of marine ice by seawater within suture zones would enable cracks to propagate upwards, possibly to sea level in the absence of back stress [*Rist et al.*, 2002]. Weakening of the suture zones has been proposed as a possible factor in the destabilization of Larsen B [*Glasser and Scambos*, 2008], and the reduction of marine ice formation specifically suggested as part of the process [*Holland et al.*, 2009].

[13] Finally, our earlier analysis of Larsen B showed that the ice shelf 18 months before its collapse had been traversed by strong, lateral speed gradients extending from the grounding line to the front along the suture zones (Figure 2, inset). These features corresponded closely to where the ice shelf broke up in 2002 [*Khazendar et al.*, 2007]. Indeed, rheological analyses underlined the role played by such bands of strong shearing and weakness in destabilizing the ice shelf [*Vieli et al.*, 2006; 2007; *Khazendar et al.*, 2007]. Hence, a further finding of this work is the absence of such strong gradient lines from the speed field of Larsen C

(Figure 2). This suggests a more kinematically stable ice shelf than Larsen B at the eve of its collapse.

5. Conclusions

[14] We conclude that although the Larsen C Ice Shelf is likely not on the brink of collapse at present, it is undergoing significant and rapid change toward possible destabilization. Specifically, we find that over 8 years the ice shelf underwent sustained acceleration that is related spatially to thinning zones and surrounding fractures. We unveil the structural heterogeneity of the ice shelf including relatively less stiff ice in the suture zones down-flow from grounding-line promontories and stiff ice in the northernmost areas of marine ice filling and healing of fracture. Continued acceleration that overlaps with thinning areas of the ice shelf, combined with susceptible suture zones and marine ice, presage destabilization if Larsen C were to evolve similarly to Larsen B.

References

Cook, A. J., and D. G. Vaughan (2010), Overview of areal changes of the ice shelves on the Antarctic Peninsula over the past 50 years, *Cryosphere*, 4, 77–98, doi:10.5194/tc-4-77-2010.

Glasser, N. F., and T. A. Scambos (2008), A structural glaciological analysis of the 2002 Larsen B ice shelf collapse, *J. Glaciol.*, 54, 3–16, doi:10.3189/002214308784409017.

Glasser, N. F., B. Kulessa, A. Luckman, D. Jansen, E. C. King, P. R. Sammonds, T. A. Scambos, and K. C. Jezek (2009), Surface structure and stability of the Larsen C ice shelf, Antarctic Peninsula, *J. Glaciol.*, 55, 400–410, doi:10.3189/002214309788816597.

Griggs, J. A., and J. L. Bamber (2009), Ice shelf thickness over Larsen C, Antarctica, derived from satellite altimetry, *Geophys. Res. Lett.*, 36, L19501, doi:10.1029/2009GL039527.

Haran, T., J. Bohlander, T. Scambos, and M. Fahnestock (2005), MODIS mosaic of Antarctica (MOA) image map, digital media, Natl. Snow and Ice Data Cent., Boulder, Colo.

Holland, P. R., H. F. J. Corr, D. G. Vaughan, A. Jenkins, and P. Skvarca (2009), Marine ice in Larsen Ice Shelf, *Geophys. Res. Lett.*, 36, L11604, doi:10.1029/2009GL038162.

Jansen, D., B. Kulessa, P. R. Sammonds, A. Luckman, E. C. King, and N. F. Glasser (2010), Present stability of the Larsen C ice shelf, Antarctic Peninsula, *J. Glaciol.*, 56, 593–600, doi:10.3189/002214310793146223.

Khazendar, A., and A. Jenkins (2003), A model of marine ice formation within Antarctic ice shelf rifts, *J. Geophys. Res.*, 108(C7), 3235, doi:10.1029/2002JC001673.

Khazendar, A., E. Rignot, and E. Larour (2007), Larsen B Ice Shelf rheology preceding its disintegration inferred by a control method, *Geophys. Res. Lett.*, 34, L19503, doi:10.1029/2007GL030980.

Khazendar, A., E. Rignot, and E. Larour (2009), Roles of marine ice, rheology, and fracture in the flow and stability of the Brunt/Stancomb-Wills Ice Shelf, *J. Geophys. Res.*, 114, F04007, doi:10.1029/2008JF001124.

Larour, E., E. Rignot, I. Joughin, and D. Aubry (2005), Rheology of the Ronne Ice Shelf, Antarctica, inferred from satellite radar interferometry data using an inverse control method, *Geophys. Res. Lett.*, 32, L05503, doi:10.1029/2004GL021693.

Morris, E. M., and D. G. Vaughan (2003), Spatial and temporal variation of surface temperature on the Antarctic Peninsula and the limit of viability of ice shelves, in *Antarctic Peninsula Climate Variability: Historical and Paleoenvironmental Perspectives*, *Antarct. Res. Ser.*, vol. 79, edited by E. Domack et al., pp. 61–68, AGU, Washington, D. C.

Rack, W., C. S. M. Doake, H. Rott, A. Siegel, and P. Skvarca (2000), Interferometric analysis of the deformation pattern of the northern Larsen Ice Shelf, Antarctic Peninsula, compared to field measurements and numerical modeling, *Ann. Glaciol.*, 31, 205–210, doi:10.3189/172756400781819851.

Riedl, C., H. Rott, and W. Rack (2004), Recent variations of Larsen Ice Shelf, Antarctic Peninsula observed by Envisat, in *Proceedings of the 2004 Envisat and ERS Symposium, 6–10 September 2004, Salzburg, Austria*, *Eur. Space Agency Spec. Publ., ESA SP-572*.

Rignot, E., G. Casassa, P. Gogineni, W. Krabill, A. Rivera, and R. Thomas (2004), Accelerated ice discharge from the Antarctic Peninsula following the collapse of Larsen B ice shelf, *Geophys. Res. Lett.*, 31, L18401, doi:10.1029/2004GL020697.

Rist, M. A., P. R. Sammonds, H. Oerter, and C. S. M. Doake (2002), Fracture of Antarctic shelf ice, *J. Geophys. Res.*, 107(B1), 2002, doi:10.1029/2000JB000058.

Rommelaere, V., and D. MacAyeal (1997), Large-scale rheology of the Ross Ice Shelf, Antarctica, computed by a control method, *Ann. Glaciol.*, 24, 43–48.

Rott, H., P. Skvarça, and T. Nagler (1996), Rapid collapse of northern Larsen ice shelf, *Antarct. Sci.*, 271, 788–792.

Scambos, T., C. Hulbe, M. Fahnestock, and J. Bohlander (2000), The link between climate warming and break-up of ice shelves in the Antarctic Peninsula, *J. Glaciol.*, 46, 516–530, doi:10.3189/172756500781833043.

Shepherd, A., D. Wingham, T. Payne, and P. Skvarca (2003), Larsen ice shelf has progressively thinned, *Science*, 302, 856–859, doi:10.1126/science.1089768.

Skvarca, P., H. De Angelis, and A. Zakrajsek (2004), Climatic conditions, mass-balance, and dynamics of Larsen B Ice Shelf, Antarctic Peninsula, prior to collapse, *Ann. Glaciol.*, 39, 557–562, doi:10.3189/172756404781814575.

Vieli, A., A. J. Payne, Z. Du, and A. Shepherd (2006), Numerical modeling and data assimilation of the Larsen B ice shelf, Antarctic Peninsula, *Philos. Trans. R. Soc. A.*, 364, 1815–1839, doi:10.1098/rsta.2006.1800.

Vieli, A., A. J. Payne, A. Shepherd, and Z. Du (2007), Causes of precollapse changes of the Larsen B ice shelf: Numerical modeling and assimilation of satellite observations, *Earth Planet. Sci. Lett.*, 259, 297–306, doi:10.1016/j.epsl.2007.04.050.

A. Khazendar, E. Larour, and E. Rignot, Jet Propulsion Laboratory, California Institute of Technology, 4800 Oak Grove Dr., Pasadena, CA 91109, USA. (ala.khazendar@jpl.nasa.gov)